Interactive Color Design Based on AR Virtual Implantation Technology Between Users and Artificial Intelligence

Jun Ma[1], Ying Chen[2]*
School of Visual Communication Design, Luxun Academy of Fine Arts, Dalian City, 116650, China[1]
School of Media and Animation, Luxun Academy of Fine Arts, Dalian, 116650, China[2]

***Abstract*—To achieve user interactive color design, this study takes furniture color interactive design as an example, introduces artificial intelligence and augmented reality virtual implantation technology, allowing users to design furniture colors and styles according to their own ideas. By improving cyclic consistency to generate adversarial networks, furniture image style transfer is carried out, and indoor feature point classification and virtual model registration are carried out through density based spatial clustering and other methods to design an unlabeled augmented reality furniture system. The results showed that compared to other methods, the improved cyclic consistency generation adversarial network had a higher structural similarity value. In the zebra to horse image, the structural similarity value was 0.987, which was 0.018 higher than the algorithm before improvement. The registration effect of density-based spatial clustering algorithm was good, with a shorter time consumption in different scenarios, and a maximum time consumption of 0.308 seconds in occluded composite scenes. The performance of the drawing component is good, with each process of tracking threads taking less than 20ms. The research method not only satisfies users in designing furniture colors and styles, but also enhances their experience.**

Keywords*—Artificial intelligence; AR virtual implantation technology; color; style transfer; furniture

I. Introduction

The rapid development of information technology has advanced the field of human-computer interaction (HCI) research and enhanced the user experience. However, in the home furnishing industry, there are still shortcomings in the development of human-machine interaction. Users have not been able to achieve interactive design for furniture colors and styles according to their own needs, resulting in furniture colors and other aspects that do not match the home environment [1-3]. Augmented reality (AR) virtual implantation technology (AR-VIT) can solve this problem, providing users with a better interactive experience and significantly improving their sense of participation [4-6]. The emergence of artificial intelligence (AI) technology has driven the development of image style transfer (IST), enabling personalized design to be realized. When designing indoor furniture, choosing this technology is beneficial for real-time migration and adjustment of furniture style, allowing users to adjust colors, textures, and other conditions according to their preferences to meet their needs. In this regard, in furniture color design, to achieve user interaction, this study introduces AR-VIT and uses Cycle-Consistent generative adversarial networks (CycleGAN) to transfer home style to meet the needs of user interactive color design and improve user experience. The study is divided into five sections. Section II is a literature review that introduces the research status of domestic and foreign scholars on furniture design, CycleGAN algorithm, and AR-VIT. Section III involves IST, virtual model registration, fusion of 3D reconstruction algorithms, and virtual real fusion of furniture models. Section IV conducts result analysis to study the image clustering effect and the application of AR-VIT. Section V summarizes the research methods, pointing out shortcomings and future research directions. The contributions of the research are as follows: (1) the study introduced artificial intelligence and augmented reality virtual implantation technology, enabling users to interactively design furniture colors and styles based on personalized needs. (2) By optimizing loop consistency, the improved network proposed in this study exhibits higher structural similarity values in furniture image style transfer. (3) We have researched, designed, and implemented a label free augmented reality furniture system that can integrate user designed furniture styles into the actual environment in real-time, enhancing the user experience. The abbreviation table used in the study is shown in Table I.

TABLE I. Related Time Consumption

Full name	Abbreviation
Human-computer interaction	HCI
Augmented reality	AR
Augmented reality virtual implantation technology	AR-VIT
Artificial intelligence	AI
Image style transfer	IST
Cycle-Consistent generative adversarial networks	CycleGAN
Features from accelerated segment test	FAST
Random sample consensus	RANSAC
Parallel tracking and mapping	PTAM
Bundle adjustment	BA
Sum of squared differences	SSD
Multi-modal unsupervised image to image translation	MUNIT
Peak signal-to-noise ratio	PSNR
Structural similarity	SSIM
Inception score	IS
Normalized mutual information	NMI

II. Related Work

In the field of HCI, color interactive design is a part of it. However, in the field of furniture design, the user experience in furniture color and other aspects still needs to be improved. Ge S et al. conducted research on digital design methods for furniture cultural tourism exhibition platforms to improve their design level, based on multimedia networks. They collected and summarized data on Jinzuo furniture from different platforms, and divided furniture genres. After analysis, it was found that design methods can promote the improvement of platform design level [7]. Jiang L et al. studied adolescents and children to understand whether they were influenced by their own color preferences when choosing furniture. They analyzed the color preferences of different functional furniture at different ages. Tests have found that their color preferences can affect the selection of different types of furniture [8]. In the process of designing living room furniture, Nasir EB conducted a specific analysis of the application of design thinking in the design of living room furniture for students. The results showed that under the influence of design thinking, it was beneficial to understand the vague needs of users and had a positive promoting effect on design practice [9]. In the process of studying library furniture, Parvez M S et al. faced the problem of matching its size with student body measurements, conducted experimental settings, collected relevant data on students and home design, and compared them. The mismatch between these two types of data was more pronounced, which would be detrimental to the growth and development of students [10]. Lee I J et al. introduced AR technology and conducted comparative experiments to promote the understanding of 3D space for novice carpenters. With the help of AR, novice carpenters could better understand 3D space and have a higher level of mastery of complex mortise and tenon structures [11].

Liu X et al. designed and optimized the CycleGAN algorithm for unsupervised training in image dehazing, based on the relevant generator. Comparative analysis showed that this method had a better visual effect on image processing [12]. Chen et al. introduced the CycleGAN algorithm in spatio-temporal image fusion to address the issue of insufficient spatial information in images, and based on this, proposed a corresponding fusion framework. This model simulated the generation and processing of images, and input them into the constructed framework. After verification, the application effect of the proposed method was good [13]. In the process of studying Earth observation applications, Soto P J et al., faced with insufficient training data, chose the CycleGAN algorithm and improved the adaptability of the research object through nonlinear mapping functions. The proposed method could effectively solve the domain transfer problem in remote sensing applications [14]. Angrini L M and others faced the problem of poor mathematical thinking among students and conducted experiments on flat shape design using AR technology based on Unity 3D software. It randomly selected students for testing and interviews, and conducted result analysis. With the assistance of AR, students' mathematical and computational abilities had been significantly improved [15]. Ahmad H et al. focused on consumers and selected respondents to analyze their potential travel destinations during the pandemic, collecting their views on the impact of AR on tourism behavior. Statistical data showed that AR technology had a certain degree of impact on the travel intentions of consumers [16].

In summary, in the design of furniture styles and other aspects, most of them tend to focus on the specific design situation of furniture, with less emphasis on combining AI and AR-VIT, and there has been no research on user interaction color design. The CycleGAN algorithm has shown good performance in IST, which helps users design furniture styles. In addition, AR-VIT can overlay virtual objects into the actual environment, which is beneficial for furniture display. Therefore, to achieve interactive design of furniture styles such as color and texture for users, this study cites the CycleGAN algorithm and AR-VIT for furniture interactive design. Compared to previous research, this study has developed an unlabeled augmented reality system, overcoming the limitations of using artificial markers and applying it to the furniture field. The advantages and disadvantages analysis of different methods are shown in Table II.

TABLE II. Analysis of Advantages and Disadvantages of Different Methods

Author	Technique/Method	Advantages	Disadvantages
Ge et al.	Digital Design	Enhances platform design	Limited application in interactive design
Jiang et al.	Color Preference Study	Identifies impact of color preferences	Limited generalizability
Nasir EB	Design Thinking Application	Positively promotes design practice	Lacks technical application details
Parvez et al.	Furniture Size Matching	Highlights mismatch issues beneficial for student development	Restricted to specific settings
Lee et al.	AR Technology Application	Improves mastery of complex structures	Limited to novice carpenters
Liu et al.	CycleGAN Optimization	Better visual effects in image processing	Application scenarios not detailed
Chen et al.	CycleGAN in Image Fusion	Proposes a fusion framework with good application effects	Performance in practical scenarios not specified
Soto et al.	CycleGAN in Remote Sensing	Solves domain transfer issues effectively	Limited to remote sensing domain
Angrini et al.	AR for Computational Thinking	Significantly enhances students' abilities	Limited scope and generalizability
Ahmad et al.	Impact of AR on Tourism Behavior	Shows impact of AR on travel intentions	Limited to pandemic context

III. Interactive Design Based on AI and AR-VIT

To achieve interactive design of furniture styles such as color and texture, this study improves the CycleGAN algorithm to assist users in personalized design of furniture styles. Using AR-VIT, indoor feature point classification and virtual model registration are carried out through density-based spatial clustering of applications with noise DBSCAN and other methods, and an unlabeled augmented reality furniture system design is carried out.

A. IST based on Improved CycleGAN Algorithm

The development of the real estate market has led to the rapid prosperity of the furniture industry, but users still choose furniture using traditional methods. When users are not satisfied with the color, texture, etc. of furniture, it often means that the product transaction has failed, or when the purchased furniture arrives at home, there is a situation where it does not meet the expected effect. Therefore, to achieve interactive design of furniture color among users, this study conducts furniture IST based on user needs to change furniture color. The CycleGAN algorithm is introduced in this study, and its generator structure is Fig. 1.

In Fig. 1, for the CycleGAN algorithm generator, its transformation network contains six residual blocks, and its encoding network has three convolutional layers. Due to the incomplete style transfer and other issues in generating furniture images using this algorithm, this study improves the algorithm by optimizing its generator, discriminator, and loss function. The main architecture of the improved algorithm is the U-Net network, and nine residual blocks are added to the bottom of the network to promote sufficient transformation of image style. In improving the CycleGAN algorithm, its discriminative network has two discriminators. Different discriminators discriminate from different receptive fields to achieve higher network discrimination performance. In the improvement of the loss function, the L1 norm of the identity loss function is added, and the Wasserstein distance with gradient penalty term is introduced to rewrite the original adversarial loss function and improve the performance of the algorithm. The overall architecture of the improved CycleGAN algorithm is Fig. 2.

In Fig. 2, X and Y represent two different domains, with X being the content domain and Y being the style domain. Sample x in X and sample y in Y. x obtains sample $\hat{y}$ through the generator. D_Y is a discriminative network for Y, used to distinguish between y and $\hat{y}$ and determine the probability value of the true sample. F represents the generator from Y to X. $\hat{y}$ generates sample $\hat{x}$ through F. D_x represents the discriminative network of X, and x and $\hat{x}$ can be distinguished through D_x. To maintain the relative balance between the generator and the discriminative network, it is necessary to alternate training between the two, with the images being trained from X to Y and then to X, thus forming a loop. Specifically, to design two generators to improve the CycleGAN algorithm, with the same structure. By adopting this symmetrical structure, feature maps that are completely aligned with the content domain and style domain can be obtained. Overall, the structure of the generator is Fig. 3.

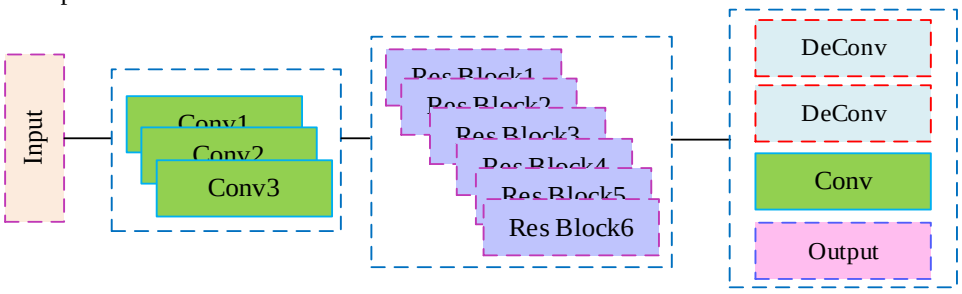

Fig. 1. Related structures.

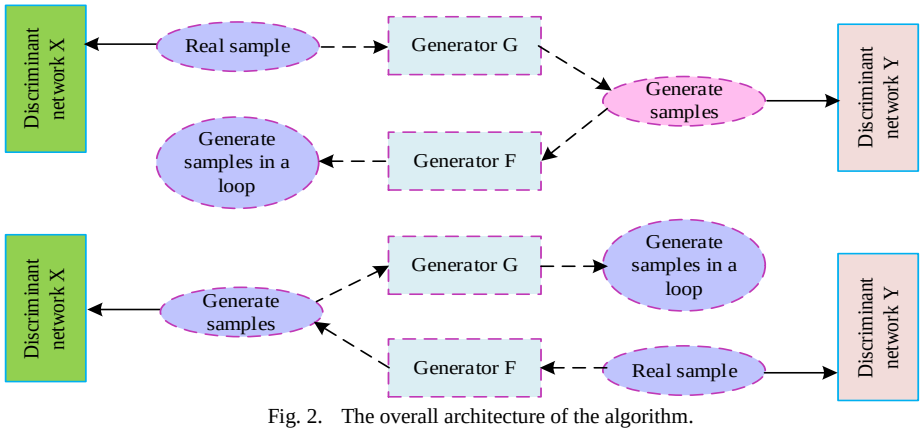

Fig. 2. The overall architecture of the algorithm.

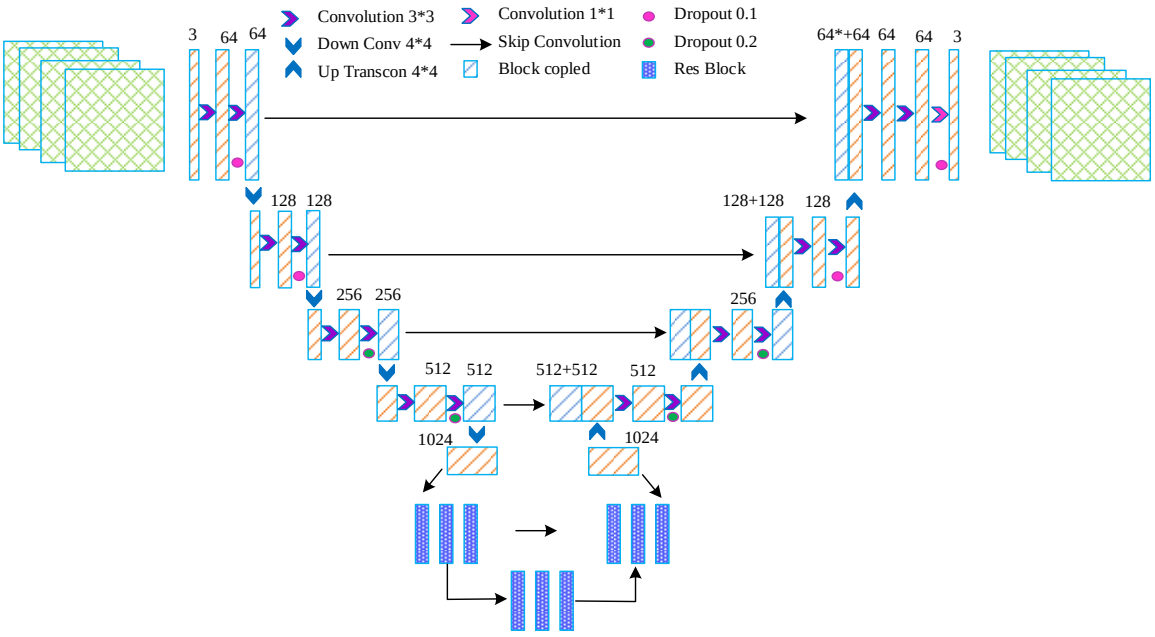

Fig. 3. Encoding network and decoding network.

In Fig. 3, the encoding network and decoding network represent the contraction path and expansion path of the U-Net network, respectively. In an encoding network, the size of the input image is 3 * 256 * 256, and the output is a feature map with a size of 1024 * 30 * 30. The sliding step size of the convolutional layer is set to 1, its filling amplitude is 1, and its convolution kernel is 3 * 3. Under the influence of this convolutional layer, the input image is processed into a feature map of 64 * 256 * 256. Due to the fact that selecting either the maximum pooling layer or the average pooling layer during down-sampling can result in significant loss of feature information. In the face of this problem, this study sets the convolution kernel to a size of 4 * 4, with a sliding step size of 2 and a filling amplitude of 1, respectively. In this case, it can be ensured that the number of output channels remains unchanged and the feature map size is halved. To encode and process images according to the two designed convolution kernels. The convolutional kernel size of the last down-sampling convolutional layer is 5 * 5, with a sliding step size and filling amplitude of 1 to obtain the final feature map. The image serves as the input of the transformation network, and the final output feature map size remains unchanged. Among them, in the residual block, a mirror is filled with a filling amplitude of 1, and the edge information of the feature map is saved as much as possible, making the feature map size 1024 * 32 * 32. Under the influence of a convolutional layer containing 3 * 3 convolution kernels, the size of the feature map changes to 1024 * 30 * 30. Repeating the image filling and convolutional layer processing, with the same parameter settings, to make the feature map size 1024 * 30 * 30 again. Using ReLu activation function and instance normalization layer to input the obtained feature map into the decoding network. Its output is the image after style transfer. During this period, feature maps and two different sizes of convolutional layers are concatenated using skip connections, ultimately enabling image reconstruction. The sizes of these two types of convolutional layers are 5 * 5 and 3 * 3, respectively.

Design of discriminator: It involves adding discriminator D_1 to the original discriminator PatchGAN D_2. The two discriminators have the same structure, but there is a difference in their input feature sizes. The former is 3 * 256 * 256, while the latter is 3 * 128 * 128. Calculating the mean probability value of two discriminators, and the result obtained is the final output probability value. To design the loss function, and the loss function L_{GAN} from X to Y is Eq. (1).

$$L_{GAN}(G,D_Y,X,Y)=E_{x\sim P_G}[D_Y(x)]-E_{x\sim P_{data}}[D_Y(y)]+\lambda \underset{\hat{x}\sim P_{\hat{x}}}{E}[(\|\nabla_{\hat{x}}D_Y(\hat{x})\|_2-1)^2] \quad (1)$$

In Eq. (1), the distribution of X and Y is set to $x\sim P_{data}$ and $y\sim P_{data}$, respectively. P represents the smallest rectangular plane of the feature points, which belongs to the initial plane. After passing G, the potential distribution $y\sim P_G$ of X 's image can be obtained. $\underset{\hat{x}-P_{\hat{x}}}{E}$ represents the gradient penalty term. Constraining the gradient around 1 to satisfy the Lipschitz condition for the discriminator. The penalty coefficient is set to λ, and the corresponding distribution $\hat{x}-P_{data}$ can be obtained through $x\sim P_{data}$ and $y\sim P_{data}$.

$$L_{GAN}(G,D_X,Y,X)=E_{y\sim P_G}[D_X(y)]-E_{y\sim P_{data}}[D_Y(y)]+\lambda \underset{\hat{y}\sim P_{\hat{y}}}{E}[(\|\nabla_{\hat{y}}D_X(\hat{y})\|_2-1)^2] \quad (2)$$

Eq. (2) is the adversarial loss function from Y to X.

$$L_{identity}(G,F)=E_{y\sim P_{data}}[\|G(y)-y\|_1]+E_{x\sim P_{data}}[\|F(x)-x\|_1] \quad (3)$$

In Eq. (3), $L_{identity}(G,F)$ represents the identity loss function.

$$L(G,F_x,D_X,D_Y)=L_{GAN}(G,D_Y,X,Y)+L_{GAN}(F,D_X,Y,X)+\lambda_i L_{identity}+\lambda_c L_{cyc}(G,F) \quad (4)$$

In Eq. (4), $L(G,F_x,D_x,D_Y)$ is the total loss function. $L_{cyc}(G,F)$ represents the cyclic consistency loss function. λ_i and λ_c are hyper-parameters. Adjusting the proportion of the loss function to the total loss function through these parameters.

B. Furniture System Based on DBSCAN Algorithm and AR-VIT

After completing the furniture style design, AR-VIT is introduced to conduct research on furniture stacking in actual environments. The first step is to register the virtual model, as shown in Fig. 4.

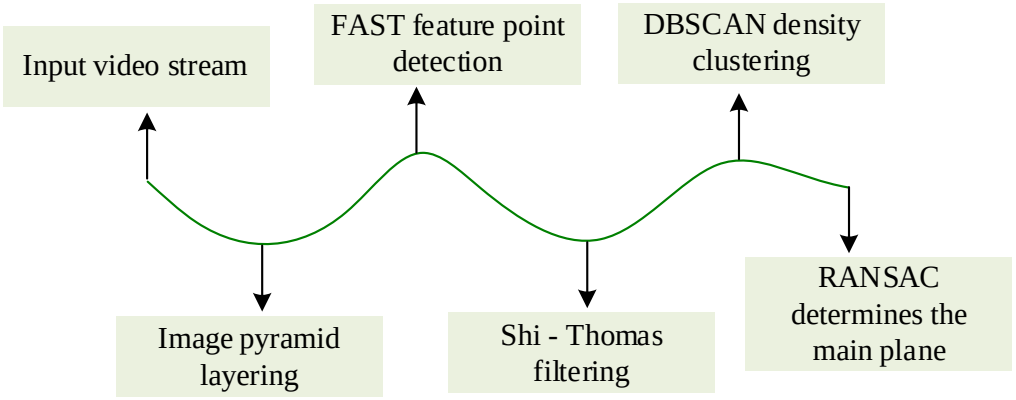

Fig. 4. Registration process.

In Fig. 4, the camera captures the video stream and performs pyramid layering on it. Different image layers correspond to different scales. The Features from accelerated segment test (FAST) algorithm has been selected to detect layered image features. Definition of corner: If the difference between a pixel and a large number of neighboring pixels exceeds a predetermined threshold, there is a certain probability that the pixel belongs to the corner. The relevant formula is Eq. (5).

$$N = \sum_{x' \forall (circle(p))} \left| I(x') - I(p) \right| > \varepsilon_d \tag{5}$$

In Eq. (5), x' represents the pixels on the circumference, and $I(x')$ represents the grayscale value of x'. The center point is p and the radius is r. The threshold for grayscale difference is set to ε_d, the adjustable parameter for the algorithm is set to N, and N is set to 10. When there is more than one feature point in the region, to delete the feature points with smaller response values. Calculating the feature point score S: In the feature point set V, assuming the existence of point c, its score is S_c. At point c, there is a neighborhood with a size of $s*s$. There is an arbitrary feature point l in this region, and if S_l exceeds S_c, point l is treated as a local maximum. Iterating other feature points in V in this way. The selection of the area with the densest indoor feature points is carried out by constructing a virtual object display main plane in that area, and then classifying feature points using the DBSCAN algorithm. To achieve higher operational efficiency, the size of the clustering dataset is reduced by setting its feature point data to 500. Datasets with a scale less than 500 are directly clustered, otherwise the score of feature points is calculated using the Shi-Thomas algorithm. According to the order of scores from high to low, the top 500 points are selected for clustering. During the operation of the DBSCAN algorithm, all sample points are scanned first. If the number of points within the threshold Eps radius range of a certain sample point exceeds the threshold $MinPts$ of the number of samples in the region centered on that point with a radius of Eps, then that point is selected into the core point list. Summarizing the points with the highest density to obtain the corresponding temporary cluster. Merging all temporary clusters to determine the final cluster. In the dataset, filtering out error points and treating them as noise points to avoid their impact on clustering results. After the feature point clustering is completed, the main plane of the virtual object is established for display.

$$q = \begin{cases} reserve, if\ q \in C_{\max} \\ delete, otherwise \end{cases} \tag{6}$$

In Eq. (6), q represents the feature points, and the cluster with the highest number of feature points after clustering is set to $C_{\max}$. At the location of $C_{\max}$, to establish the main plane using random sample consensus (RANSAC), which is a rectangle. Choosing the parallel tracking and mapping (PTAM) algorithm to ensure real-time tracking of virtual objects under changing indoor environments. Before this, camera calibration is performed. This study selects a pinhole camera imaging model and calibrates the camera using the Zhang calibration method to obtain the internal and external parameters of the camera. The calibration template is in black and white chessboard format. During the calibration process, 4 frames of images need to be collected from different angles. The main module of PTAM consists of two parts: drawing thread and tracking thread. The drawing thread process is Fig. 5.

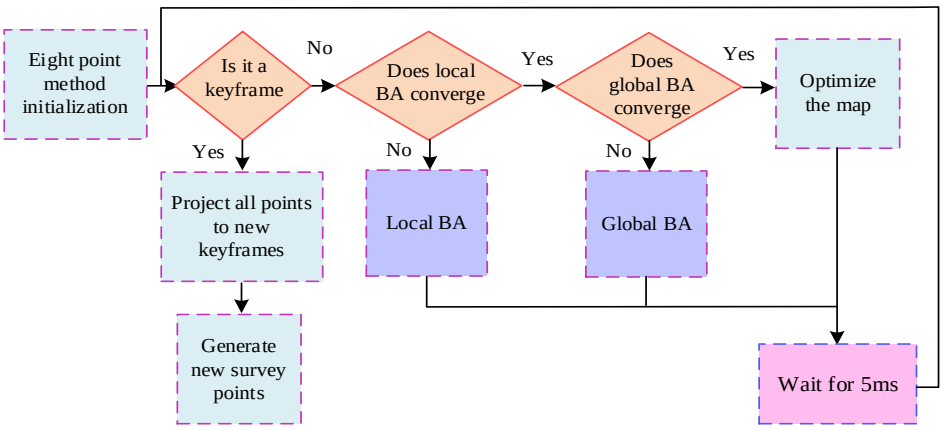

Fig. 5. Drawing thread process.

In Fig. 5, the first step is to manually set two keyframes and initialize them. When the camera deviates from the initial pose, the camera determines the current keyframe. It needs to have good tracking performance, contain a large number of feature points, and have sufficient duration. The interval between the image frame and the previous keyframe should be greater than 20 frames. In addition, the current frame should have sufficient distance in spatial position. When a keyframe is determined, the map information is updated based on the world points in that frame, combined with the original world points. Conversely, the map information is optimized using the bundle adjustment (BA) method. In local BA optimization, only the newly added last 5 keyframes and their world points are considered. The constraint is that other keyframes that can observe the world point are not optimized. In global BA optimization, all keyframes and their map points are optimized. During idle time, the drawing thread optimizes the map through old keyframes. To process outliers, treating them as new world points when they can be observed and converge, and adding them to the map. Through this approach, it is possible to prevent the loss of virtual furniture tracking and improve system accuracy. The process of tracking threads is Fig. 6.

In Fig. 6, the input image is layered into four pyramid layers, and the feature points of each layer are extracted using the FAST algorithm. The DBSCAN algorithm is used to cluster the feature points. After initializing the map, based on the initial two keyframes determined, feature points are selected through sum of squared differences (SSD) block matching (two frame images). Calculating the homography matrix between two frames, decomposing it into a rotation translation matrix, and treating it as the initial pose.

$$SSD(u,v) = Sum\left\{\left[left(u,v) - right(u,v)\right]^2\right\} \tag{7}$$

In Eq. (7), u and v represent the u-axis and v-axis of the pixel coordinate system, respectively. These two coordinate axes are parallel to the x"-axis and y"-axis of the image's physical coordinate system, respectively. The smallest difference in this equation is the best matching block. The normalized coordinates of the feature points in the initial two frames are set to $\boldsymbol{x}_1$ and $\boldsymbol{x}_2$, and the formulas involved in these two coordinates are shown in Eq. (8).

$$s_1 x^*_1 = s_2 R x^*_2 + t^* \tag{8}$$

In Eq. (8), s_1 and s_2 represent the parameters of x^*_1 and x^*_2, respectively. R and t^* are the rotation translation matrix.

$$s_1 x^{*\wedge}_1 x^*_1 = s_2 x^{*\wedge}_1 R x^*_2 + x^{*\wedge}_1 t^* \tag{9}$$

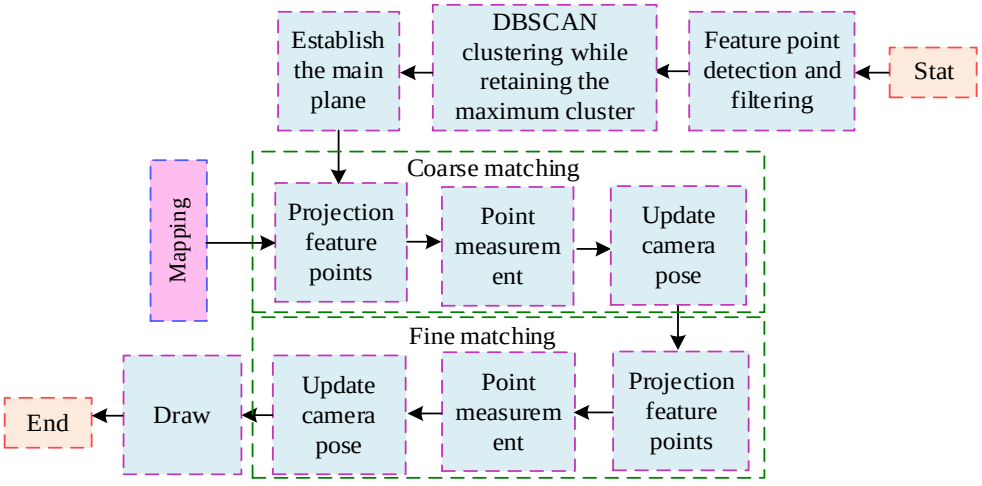

Fig. 6. Track the process of threads.

On the left side of Eq. (9), the equal sign is 0, and s_2 can be directly obtained. Based on this, s_1 can be calculated. Due to the influence of noise, R and t^* may not accurately make the left side of the equation equal to 0, so optimization is carried out through BA. The minimum objective function for local BA optimization is Eq. (10).

$$\left\{\left\{\mu_{x'} \in X'\right\}\left\{p'_z \in Z\right\}\right\} = \arg\min_{\{\{\mu\}\{p\}\}} \sum_{i \in X' \cup Y'} \sum_{i \in Z \cup S_i} Obj(i, j) \quad (10)$$

In Eq. (10), set X' consists of the current frame and its closest 4 other keyframes. In these keyframes, the observable world points are set as set Z. p'_z belongs to the world point in Z. The set of keyframes with observable world points in Z is represented as Y'. i and j are the serial number. $\mu_{x'}$ represents the element in X'. Local BA only optimizes elements in Z and X'. Calculating the initial pose of the camera. After obtaining the coordinates of the world point through triangulation, establishing the display main plane. 30-60 points in the top layer of the image pyramid are selected for coarse matching, and the world points based on the camera's pose are mapped. It is projected into the current frame to calculate the error with the current feature point. Based on the obtained results, an error optimization function is established and the camera pose is calculated. Based on the updated camera pose, to re select image points with a quantity of around 1000. Performing pose detection: The process is the same as coarse matching. Optimizing the pose by combining all points. The PTAM component completes the 3D registration of virtual furniture models to the real environment's 3D coordinate system and real-time tracking through the above process. Virtual real fusion uses user input to paste stylized images onto the surface of the constructed virtual furniture 3D model, and obtains the correct occlusion relationship. This can minimize the number of model vertices and patches, and reduce scene drawing calls, thereby achieving system performance optimization.

IV. Application Analysis of Furniture Systems Based on IST and AR-VIT

To analyze the effectiveness of IST and improve the performance of the CycleGAN algorithm, this study compared multiple algorithms with CycleGAN. By analyzing the performance of DBSCAN and PTAM algorithms, the application of the system could be evaluated.

A. Analysis of IST Results

To verify the performance of the improved CycleGAN algorithm, the Ubuntu operating system was selected with a learning rate of 0.0002. The experiment used the Horse2Zebra public dataset, $\lambda_c = 10$, $\lambda = 10$, and $\lambda_i = 1$. The comparative algorithms were the CycleGAN algorithm and the multi-modal unsupervised image to image translation (MUNIT) algorithm. The evaluation indicators were peak signal-to-noise ratio (PSNR), structural similarity (SSIM), and inception score (IS). The style transfer effect of the algorithm under different iterations analyzed is Fig. 7.

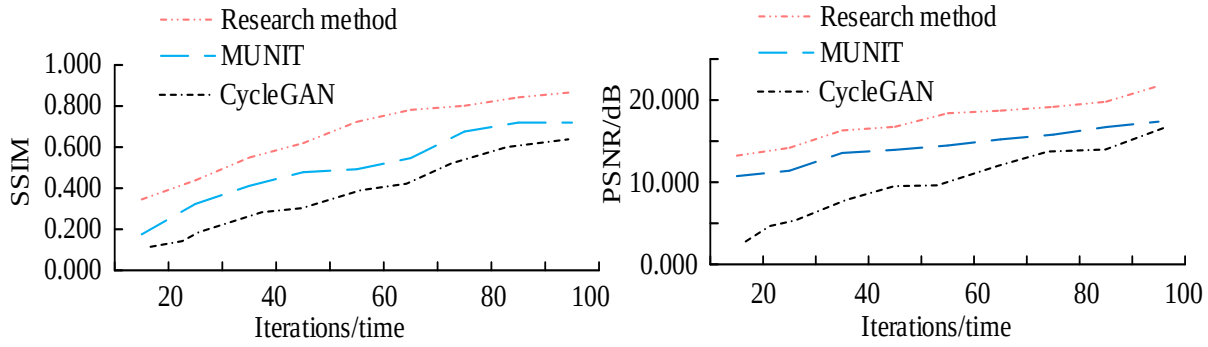

(a) SSIM values under different iteration numbers (b) PSNR values under different iteration numbers

Fig. 7. Style transfer effect.

In Fig. 7 (a), as the number of iterations increased, the SSIM value of the iterative feature effect map also increased, and the quality of the iterative map obtained by the research method was better. When the number of iterations was 35, the SSIM value of the research method was 0.547, which was 0.135 higher than the MUNIT algorithm, while the SSIM value of the CycleGAN algorithm was the smallest. When the iteration was 75, the SSIM values of the research method and MUNIT algorithm were 0.805 and 0.679, respectively. In Fig. 7 (b), the line where the research method was located was above the line where other algorithms were located. When the iteration was 45, the PSNR value of the research method was 16.201dB, which was 6.204dB higher than the CycleGAN algorithm. The results of analyzing the conversion effect between horse and zebra images are shown in Fig. 8.

In Fig. 8 (a), compared to methods such as the CycleGAN algorithm, the PSNR, SSIM, and IS of the research method were all larger. The IS value of the research method was 3.242, which was 1.635 higher than CycleGAN and 0.949 higher than MUNIT. In Fig. 8 (b), the SSIM values of the research method, CycleGAN, and MUNIT were 0.987, 0.969, and 0.955, respectively, indicating that the research method had the highest SSIM value. Therefore, the research method generated images with good quality.

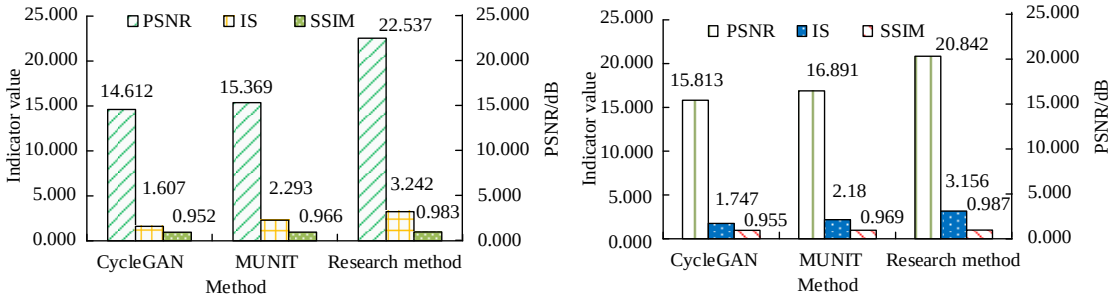

(a) Comparison result of turning horse to zebra image

(b) Comparison result of turning zebra to horse image

Fig. 8. Related comparison results.

B. *Application Analysis of Unlabeled AR Furniture System Based on DBSCAN Algorithm*

When conducting application analysis, select representative furniture design cases and demonstrate how to use artificial intelligence and augmented reality technology to customize furniture colors and styles based on personalized user needs. Collecting users' furniture design preferences, including color, style, etc., through style transfer, feature point classification and model registration, and the integration of virtual and reality, users can intuitively see the designed furniture in their living space through augmented reality technology. To analyze the performance of DBSCAN algorithm, the comparison method was K-means algorithm, and the dataset was UCI dataset. The evaluation indicators were normalized mutual information (NMI) and accuracy, and the comparison results are shown in Fig. 9.

In Fig. 9 (a), due to different datasets, there were differences in the accuracy of the same algorithm. In the glass_5 dataset, the accuracy of the DBSCAN algorithm was 0.784, which was 0.187 higher than the K-means algorithm. The maximum accuracy on other datasets was 0.854, which was also higher than the K-means algorithm. In Fig. 9 (b), overall, compared to the K-means algorithm, the DBSCAN algorithm had a larger NMI value. In the Dermatology dataset, the NMI values of DBSCAN algorithm and K-means algorithm were 0.345 and 0.082, respectively. Therefore, the DBSCAN algorithm had a good clustering effect and performance. This study analyzed the registration effect of the DBSCAN algorithm by constructing corresponding main planes at chessboard positions obstructed by objects such as packaging boxes and brochures. Table III shows the display effect.

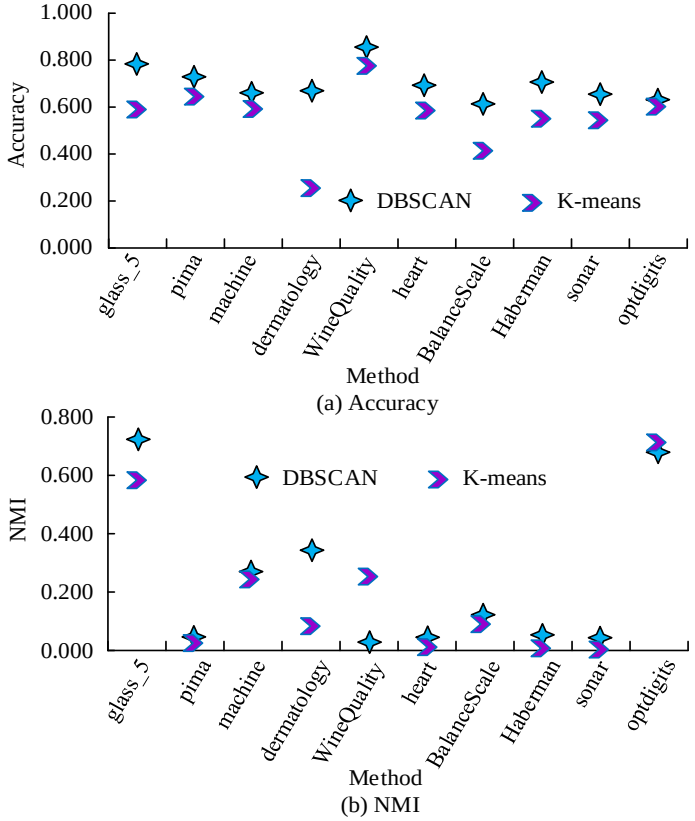

(a) Accuracy

(b) NMI

Fig. 9. Clustering results of different algorithms.

TABLE III. REGISTRATION EFFECT OF THE ALGORITHM

Scene	Number of environmental characteristic points/piece	Maximum number of points in the cluster/number	Time consumption/s
Black and white chessboard	119	106	0.156
Packaging box	158	95	0.180
Occlusion composite scene	251	169	0.308
Brochure	108	80	0.090

In Table III, the time consumption of algorithms varied depending on the scenario. Compared to other scenes, occluding composite scenes took up to 0.308 seconds, which was 0.218 seconds more than brochure scenes. Therefore, the real-time performance of the virtual object registration module was good. Table IV shows the time consumption of the drawing and tracking threads in the PTAM component.

In Table IV, when the number of keyframes was less than 50, local BA optimization and global BA optimization took less time, which were 170ms and 381ms, respectively. As the number of keyframes increased, the drawing thread's time consumption increased. When the key frame rate was between 100 and 149 frames, the global BA optimization took 6900ms. Overall, compared to other processes, the feature point measurement process took more time. When in the living room, projecting feature points took 3.5ms, which was 6.3ms less than the feature point measurement process in the same environment. Overall, each process of tracking threads took less than 20ms. Overall, the performance of PTAM components was good. Twenty users were randomly selected and rated on a scale of 1-5. The satisfaction evaluation data of the system application was collected through a survey questionnaire, as shown in Fig. 10.

In Fig. 10, compared to before system optimization, the optimized user satisfaction was higher. Overall, the user satisfaction score ranged from 3.50 to 5.00. Among them, after system optimization, the average user satisfaction score was 4.43 points, which was 0.30 points higher than before system optimization. Therefore, the application effect of the constructed AR system was outstanding.

TABLE IV. RELATED TIME CONSUMPTION

Stage	Keyframes/Frame		Local BA optimization/ms	Global BA optimization/ms
Drawing Thread	2-49		170	381
	50-99		277	1700
	100-149		445	6900
Tracking threads	Flow	Living room/ms	Bedroom 1/ms	Kitchen/ms
	Projection feature points	3.5	2.6	3.0
	Update camera pose	3.5	2.9	2.8
	Get keyframes	2.3	3.1	2.9
	Measurement of feature points	9.8	8.4	9.5

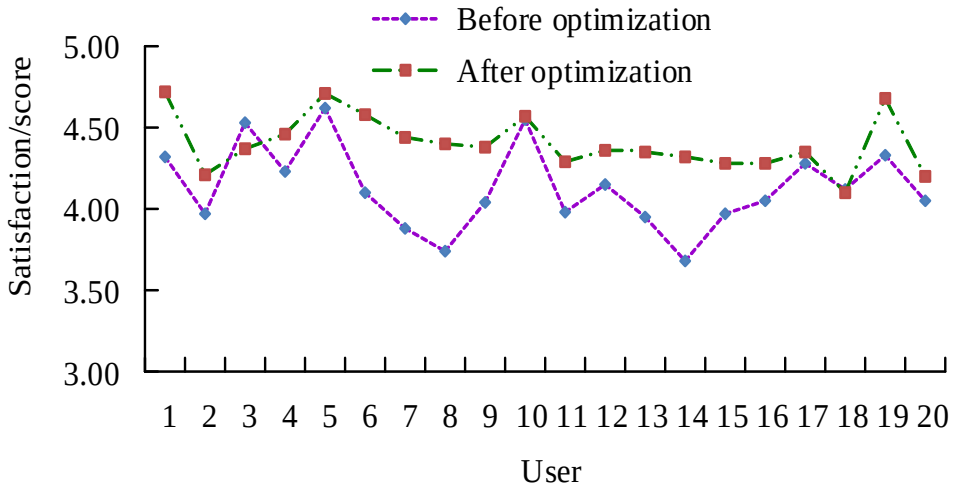

Fig. 10. User satisfaction with the system before and after optimization.

V. CONCLUSION

To achieve color interactive design for users, enhance their sense of participation and experience, this study used IST and AR-VIT to design furniture styles, achieving the goal of user color interactive design for furniture. Firstly, the CycleGAN algorithm was introduced for IST, and the overall performance of the algorithm was improved through identity loss functions and other means, making it convenient for users to design personalized furniture colors and styles. Subsequently, AR-VIT was introduced, and virtual model registration was performed using the DBSCAN algorithm, followed by the design of an unlabeled AR furniture system. The results showed that the improved CycleGAN algorithm performed better. When the number of iterations was 35, the SSIM value of the research method was 0.547, which was 0.135 higher than the MUNIT algorithm, while the SSIM value of the CycleGAN algorithm was the smallest. The IS value of the research method was 3.242, which was 1.635 higher than the CycleGAN algorithm. Compared to K-means, DBSCAN algorithm had higher accuracy and NMI. In the glass_5 dataset, the maximum accuracy of the DBSCAN was 0.854, which was higher than the K-means. In the PTAM component, the tracking thread took less time. When in the living room, the projection of feature points took 3.5ms, which was 6.3ms less than the feature point measurement process in the same environment. The user satisfaction after system optimization was relatively high, with an average satisfaction score of 4.43. Overall, the application effect of the research method is good. At present, the research method only considers the design content of color design in furniture design, and has not yet conducted targeted design for furniture appearance, structure, and material design, and cannot participate in the complete furniture design process. Subsequent research will focus on designing other aspects involved in furniture design, and integrate existing processes with other aspects to design furniture design methods that can meet more design needs and expand the scope of research methods.

REFERENCES

[1] Wang J, Pan Y. Design evaluation of parent-child interactive game furniture based on AHP-TOPSIS method. Journal of the Korea Convergence Society, 2022, 13(2): 235-248.

[2] Jarža L, Čavlović A O, Pervan S, Španić N, Klarić M, Prekrat S. Additive Technologies and Their Applications in Furniture Design and Manufacturing. Drvna industrija, 2023, 74(1): 115-128.

[3] Purohit J, Dave R.Leveraging Deep Learning Techniques to Obtain Efficacious Segmentation Results. Archives of Advanced Engineering Science, 2023, 1(1):11-26.

[4] Kumar H, Gupta P, Chauhan S. Meta-analysis of augmented reality marketing. Marketing Intelligence & Planning, 2023, 41(1): 110-123.

[5] Wu C H, Lin Y F, Peng K L, Liu, C. H. Augmented reality marketing to enhance museum visit intentions. Journal of Hospitality and Tourism Technology, 2023, 14(4): 658-674.

[6] Li M, Liu L. Students' perceptions of augmented reality integrated into a mobile learning environment. Library Hi Tech, 2023, 41(5): 1498-1523.

[7] Ge S, ** Z. Research on the Application of Digital Design of **zuo Furniture Cultural Tourism Display Platform Based on Intangible Cultural Heritage. International Journal of Communication Networks and Information Security, 2023, 15(2): 1-12.

[8] Jiang L, Cheung V, Westland S, Rhodes P A, Shen L Xu L. The impact of color preference on adolescent children's choice of furniture. Color Research & Application, 2020, 45(4): 754-767.

[9] Nasir E B. Identifying unspoken desires and demands: a collection of design ideas for living room furniture and zones. Journal of Design Thinking, 2021, 2(1): 71-84.

[10] Parvez M S, Tasnim N, Talapatra S, Kamal T, Murshed M. Are library furniture dimensions appropriate for anthropometric measurements of university students?. Journal of Industrial and Production Engineering, 2022, 39(5): 365-380.

[11] Lee I J. Using augmented reality to train students to visualize three-dimensional drawings of mortise–tenon joints in furniture carpentry. Interactive Learning Environments, 2020, 28(7): 930-944.

[12] Liu X, Zhang T, Zhang J. Toward visual quality enhancement of dehazing effect with improved Cycle-GAN. Neural Computing and Applications, 2023, 35(7): 5277-5290.

[13] Chen J, Wang L, Feng R, Liu P, Han W, Chen X. CycleGAN-STF: Spatiotemporal fusion via CycleGAN-based image generation. IEEE Transactions on Geoscience and Remote Sensing, 2020, 59(7): 5851-5865.

[14] Soto P J, Costa G, Feitosa R Q, Happ P N, Ortega M X, Noa J, Heipke C. Domain adaptation with cyclegan for change detection in the Amazon Forest. ISPRS Archives; 43, B3, 2020, 43(B3): 1635-1643.

[15] Angraini L M, Yolanda F, Muhammad I. Augmented reality: The improvement of computational thinking based on students' initial mathematical ability. International Journal of Instruction, 2023, 16(3): 1033-1054.

[16] Ahmad H, Butt A, Muzaffar A. Travel before you actually travel with augmented reality–role of augmented reality in future destination. Current Issues in Tourism, 2023, 26(17): 2845-2862.